

## Article

# Synthesis of Lipid Nanoparticles Incorporated with *Ferula assa-foetida* L. Extract

Sylwia Ludek<sup>1,2</sup> , Agata Wawrzyńczak<sup>1</sup> , Izabela Nowak<sup>1</sup>  and Agnieszka Feliczak-Guzik<sup>1,\*</sup> 

<sup>1</sup> Faculty of Chemistry, Adam Mickiewicz University in Poznań, Uniwersytetu Poznańskiego 8, 61-614 Poznań, Poland

<sup>2</sup> Cosmo Group Sp. z o.o., Jasielska 10A, 60-647 Poznań, Poland

\* Correspondence: agaguzik@amu.edu.pl

**Abstract:** Solid Lipid Nanoparticles (SLN) have been prepared by high-pressure homogenization and optimized in order to protect ferulic acid from *Ferula assa-foetida* L. extract. The influence of lipid and surfactant concentration on the mean particle size (Z-Ave), polydispersity index (PDI), and zeta potential (ZP) of SLN was analyzed. In addition, other parameters for the preparation of ferulic acid-loaded nanoparticles, such as extract concentration and variable parameters for the synthesis method used (e.g., pressure), were adjusted to obtain the smallest particle size and polydispersity index, as well as the highest value for zeta potential, which are characteristic of the stable SLN. The established formulation obtained from the optimized synthesis was composed of 6.0 wt.% of the lipid phase and 1.5 wt.% of surfactant, giving stable SLN with Z-Ave, PDI, and ZP values of  $163.00 \pm 1.06$  nm,  $0.16 \pm 0.01$ , and  $-41.97 \pm 0.47$  mV, respectively. The loading of ferulic acid from *Ferula assa-foetida* L. extract within the SLN resulted in particles with a mean size of  $155.3 \pm 1.1$  nm, polydispersity index of  $0.16 \pm 0.01$ , zeta potential of  $-38.00 \pm 1.12$  mV, and encapsulation efficiency of 27%, the latter being quantified on the basis of RP-HPLC analysis. Our findings highlight the added value of SLN as a delivery system for phenolic phytochemical compounds extracted from *Ferula assa-foetida* L.

**Keywords:** solid lipid nanoparticles; polydispersity index; zeta potential; *Ferula assa-foetida* L.; ferulic acid; HPLC



**Citation:** Ludek, S.; Wawrzyńczak, A.; Nowak, I.; Feliczak-Guzik, A. Synthesis of Lipid Nanoparticles Incorporated with *Ferula assa-foetida* L. Extract. *Cosmetics* **2022**, *9*, 129. <https://doi.org/10.3390/cosmetics9060129>

Academic Editor: Enzo Berardesca

Received: 16 November 2022

Accepted: 29 November 2022

Published: 1 December 2022

**Publisher's Note:** MDPI stays neutral with regard to jurisdictional claims in published maps and institutional affiliations.



**Copyright:** © 2022 by the authors. Licensee MDPI, Basel, Switzerland. This article is an open access article distributed under the terms and conditions of the Creative Commons Attribution (CC BY) license (<https://creativecommons.org/licenses/by/4.0/>).

## 1. Introduction

Cosmetics, since ancient times, have been attributed a huge role, being regarded as products contributing to the ideal of a beautiful body. A beautiful body was associated with the beauty of the soul, and it was believed that a beautiful person was also a noble one. Conversely, ugliness was seen as a synonym for evil and transgression [1]. Therefore, ancient man, with the use of fragrant herbs and appropriate minerals, prepared perfume oils, perfumes, and colored makeup products. In the period between antiquity and the modern era, women used elaborate beauty treatments—the texts of the visionary and mystic Saint Hildegard of Bingen contain numerous recipes for masks and moisturizing and firming creams [2].

Plants have been used by humans since the earliest times, from being a dietary fundamental to their huge role in cultural and aesthetic life. Plant motifs have been used as decorative elements of homes, tombs, and temples. However, one of their most important applications was their use in healing, everyday hygiene, and cosmetics [3].

During the present study, historical databases (papyri.info, *Thesaurus Linguae Graecae*, *Thesaurus Linguae Latinae*) were analyzed, based on which, plants with desirable care properties, used since antiquity, were selected. These plants are Silphion (Latin: *Silphium*), Arugula (*Eruca sativa* L.), and Watercress (*Nasturtium officinale*). Of the aforementioned, Silphion deserves special attention, and its properties are the focus of this paper, as ancient

sources repeatedly mention this plant in the context of many disease treatments, as well as its beautifying action.

Silphion in the medicine of the ancient world existed as a unique plant—a Cyrenian natural wonder. Its value was measured by its weight of silver, and export to the markets of the Mediterranean world was a royal prerogative. The use of this plant in the treatment of a wide variety of conditions, namely tracheal pain, tetanus, epilepsy, sciatic nerve pain, abdominal pain., and hair loss [4], made it a subject of research. According to ancient accounts, the Cyrenian species, *Silphium*, was most likely extinct. However, related species with similar properties were still used, including the identically named *Silphium*, but also: *Laserpitium*, *Hittite*, and *Asafoetida*. Muhammad ibn Zakariya al Razi (865–925) described two types of hiltit (*Silphium*)—one nicely fragrant, the other stinking [5]. The counterpart of Silphion in the modern world, in terms of morphology, is *Ferula assa-foetida* L.

The active substance present in *Ferula assa-foetida* L. is ferulic acid (IUPAC: (2E)-3-(4-hydroxy-3-methoxyphenyl)prop-2-enoic acid; commonly named 4-hydroxy-3-methoxycinnamic acid, FA). It was *Ferula foetida* L. from which this compound was first isolated and its name comes from the botanical name of this plant [6]. In 1925, FA was chemically synthesized for the first time and its structure was confirmed by spectroscopic methods [7]. This compound exhibits skin care, anti-aging, and firming properties [8]. In addition, it is known for its antioxidant and anti-inflammatory properties, as well as its whitening effect and prevention of skin discoloration caused by photoaging [9–11]. It also exhibits stabilizing properties against vitamins C and E, which in aqueous solutions become sensitive to the presence of oxygen, high temperature, and UV radiation. In addition, ferulic acid increases the effectiveness of these vitamins [12]. Moreover, the latest study showed that *Ferula assa-foetida* L. seed oil loaded into SLN exhibits a significant cell-growth suppressive impact on the line of human stem cells causing brain cancer [13]. All possible applications of ferulic acid as an ingredient in cosmetic products are shown in Figure 1.

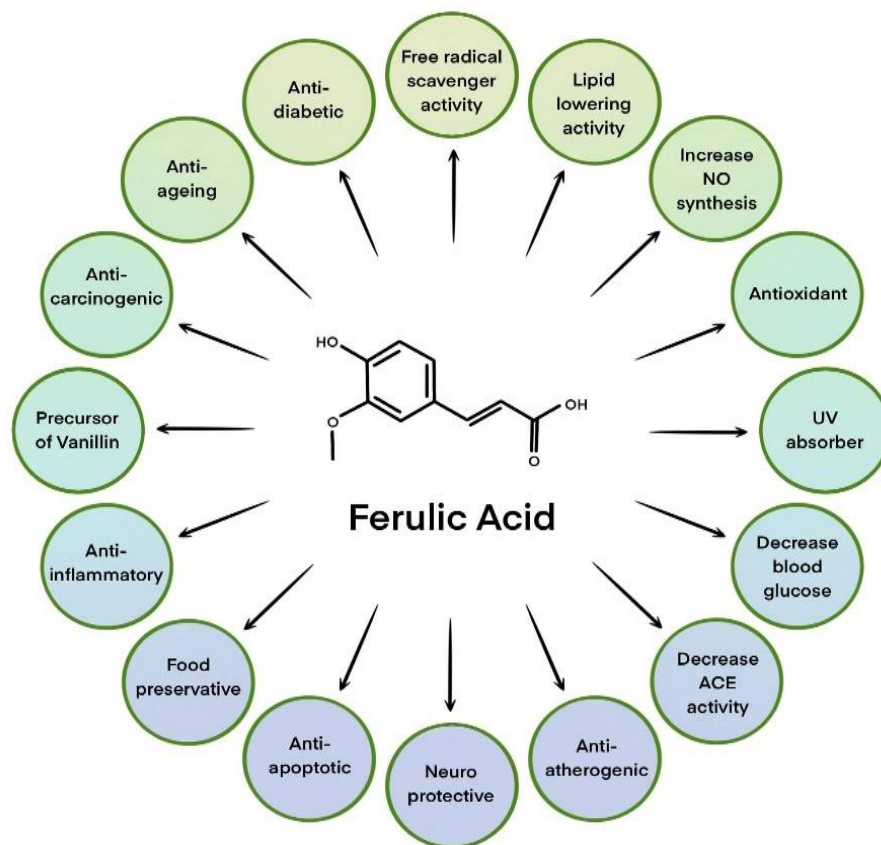
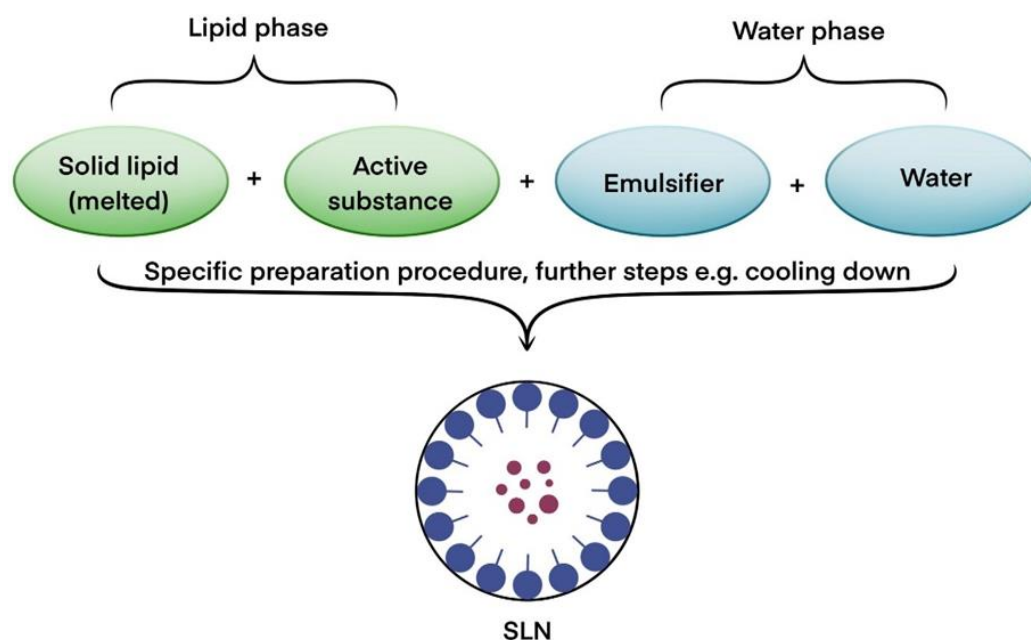


Figure 1. Various applications of ferulic acid in cosmetic products. Based on [14].

With the development of civilization and technology, the way that plants are used in cosmetics has undergone significant changes. Today, thanks to analytical methods, it is possible to accurately identify the components of plant raw materials both qualitatively and quantitatively, which allows for precise dosages of raw materials of proven quality. The use of innovative methods for processing plant raw materials (e.g., ultrasound-assisted extraction, microwave-assisted extraction, extraction using supercritical fluid, enzymatic extraction, and micellar extraction) allows the use of new plants in cosmetic formulations that were previously of little use to cosmetologists [15].

Improvement in the stability of active compounds and plant extracts is possible thanks to their incorporation into nanocapsules. The most promising carriers of active substances in cosmetic products are solid lipid nanoparticles (SLN) and nanostructured lipid carriers (NLC), which are currently under intensive study [16]. These materials have several favorable functional properties, including, but not limited to: structure based on lipids well tolerated by the human body, high stability, and the ability to carry hydro- and lipo-philic compounds [17,18]. Lipid nanoparticles are also characterized by adhesive and occlusive properties, so a protective film is formed on the surface of the skin, which reduces transepidermal water loss (TEWL) and ensures the maintenance of an adequate level of hydration [19].

Lipid nanoparticles are currently of great interest to researchers, and many publications have been devoted to them, e.g., [20–22]. SLNs were first synthesized in 1991 [23]. They are spherical particles in the size range of between 10/20 nm and 1000 nm composed of lipids that remain solid at both room temperature and body temperature. In addition, they are dispersed in an aqueous phase containing emulsifiers. Conversely, the NLC matrix is composed of both solid and liquid lipids with different spatial structures. Such lipids crystallize imperfectly and form free voids into which the active substance can be incorporated [19,24]. A single SLN structure consists of an incorporated active ingredient, a solid lipid, an emulsifier, and water [25] (Figure 2).



**Figure 2.** Block diagram of the solid structure of a lipid nanoparticle. Based on [20].

Among the methods for obtaining solid lipid nanoparticles on an industrial scale the most significant is the high-pressure homogenization method and emulsification with evaporation or solvent diffusion [26]. The most efficient method for SLN synthesis is high-pressure homogenization (HPH) [21], which involves the pre-dispersal of the lipid phase in the emulsifier solution. In a further step, cycles of high-pressure homogenization

take place several times, followed by nanoemulsion formation, cooling, and crystallization of the lipid. It should be noted that the lipid mass is pumped under high pressure (300 to 2000 bar) through a narrow space, which causes the particles to fragment to nanometer sizes. Additionally, this method sterilizes the lipid suspension by eliminating bacterial cells as a result of the high pressure. The size of the obtained nanoparticles is influenced by the type and amount of lipids and emulsifiers used, as well as the number of homogenization cycles carried out during HPH. It has been proven that the high-pressure homogenization process alone does not affect the chemical stability of the lipids underlying the nanoparticles [22]. Nevertheless, it should also be taken into account that the high pressure applied during the HPH process may induce immense shear stresses that will lead to the destruction of larger molecules of active substances incorporated into SLNs. Another limitation may be the need to apply elevated temperatures that are required to melt the lipid phase, which in turn may destabilize selected active substances. This causes some limitations in the possibility of using HPH to obtain SLNs incorporated with, for example, proteins and peptides. However, there have been reports of the successful incorporation of a peptide into the structure of an SLN using the HPH process [27].

The aim of our research was to develop stable formulations of lipid nanoparticles containing an ethanol extract of *Ferula assa-foetida* L. Encapsulation methods were selected in such a way that the physicochemical properties of the selected extract—more specifically, the active substance contained in it, namely ferulic acid—were preserved. The use of ferulic acid in skincare and cosmetic products faces some problems related to its low stability and solubility in water. These problems can be eliminated by its encapsulation into lipid nanoparticles [28].

## 2. Materials and Methods

### 2.1. Materials

Dry *Ferula assa-foetida* L. was purchased from OQEMA (Ozorków, Poland), and ethanol (96%) from Chemland (Kraków, Poland).

Solid lipids: Witepsol<sup>®</sup>H15, Softisan<sup>®</sup>601, Imwitor<sup>®</sup>900K, Dynasan<sup>®</sup>116, and Dynasan<sup>®</sup>118 were purchased from Cremer Oleo GmbH&Co. KG company (Berlin, Germany), while Compritol<sup>®</sup>888 ATO and Precirol<sup>®</sup>ATO 5 were purchased from Gattefosse (Saint-Priest, France). The surfactant Miranol Ultra used in the study was purchased from Sigma-Aldrich (Poznań, Poland). All other chemicals and solvents were of analytical purity and were used without further purification.

### 2.2. Methodology

#### 2.2.1. Preparation of Plant Extract from *Ferula assa-foetida* L.

For the preparation of the ethanol extract of *Ferula assa-foetida* L., 3 g of raw material was weighed and poured over 6 g of ethanol. The extraction process was carried out at 25 °C for 24 h, with the first 3 h involving sonication of the raw material in an ultrasonic bath (Elmasonic X-tra 50H, Elma, Germany) at 35 kHz. Then the sample was transferred to a magnetic stirrer and stirred for 18 h. Finally, the last 3 h of the extraction process again included sonication in the ultrasonic bath.

#### 2.2.2. Analysis of Active Substances Isolated from *Ferula assa-foetida* L.

The plant extract obtained according to the method described in Section 2.2.1 was analyzed using a VARIAN 4000 GC-MS gas chromatograph (Stevens Creek Blvd.; Santa Clara, CA, USA) coupled to a mass detector, equipped with an automatic sample dispenser and a VF-5 MS capillary column with an inner diameter of 0.25 mm and a length of 30 m. The flow rate of the carrier gas (helium, purity N5.0) was 1 cm<sup>3</sup>/min. The method of analysis is shown in Table 1.

**Table 1.** Method for analyzing the chemical composition of *Ferula assa-foetida* L. extract using a gas chromatograph coupled to a mass detector.

<b>Injector</b>			
Injector Temperature:	220 °C		
<b>Column</b>			
	Rate [°C/min]	Temperature [°C]	Time [min]
Temperature program:	0	80	1
	10	220	28
Total time			29

Identification and quantification of the components was based on the National Institute of Standardization and Technology (NIST) database and compared with appropriate standards.

### 2.2.3. Optimization of the Synthesis of SLN-Type Lipid Nanoparticles

#### Lipid Screening

Before the synthesis of the lipid nanoparticles, lipid selection (lipid screening) was performed to assess the miscibility of a given lipid with the selected ethanol extract. To select the most suitable lipid, lipid screening was carried out using seven different solid lipids (Table 2) with ethanol extract from *Ferula assa-foetida* L. For this purpose, 2 g of each solid lipid tested was weighed into glass vials. Then, 0.02 g of the ethanol extract was added to each vial. One by one, the vials were placed on a magnetic stirrer and their contents were heated to a temperature above the lipid melting point (Table 2). The melted lipid together with the *Ferula assa-foetida* L.–ethanol extract was stirred continuously until a homogeneous mixture was obtained. After the mixture was cooled to 25 °C, observations were recorded at specific time intervals (15 min, 30 min, 1 h, 24 h, and 72 h). The assessment of miscibility was based on observation of the coloring of the mixture of the lipid and the extract with an active substance. It is assumed that the tested extract can be incorporated into lipid nanoparticles if the solidified lipid mixture with the extract takes on a white color. Conversely, any other color of the mixture may indicate either too much extract used or the inappropriate chemical nature of the lipid relative to the active ingredient under test. As a result of the observations made on the solubility of the extract at given time intervals, the Witepsol®H15 lipid was selected for the synthesis of the SLN-type lipid nanoparticles.

**Table 2.** A list of lipids with their corresponding melting point.

Trade Name	Chemical Composition	Melting Point [°C]
Witepsol®H15	A mixture of triacylglycerols of saturated fatty acids with the addition of mono- and diacylglycerols	31–38
Softisan®601	Glycerol stearate	40–45
Imwitor®900K	Glycerol monostearate, Type II	54–64
Dynasan®116	Glycerol tripalmitate	61–65
Dynasan®118	Glycerol tristearate	70–73
Compritrol®888 ATO	Glycerol behenate (mixture of mono-, di-, and tri-)	70
Precirol®ATO 5	Glycerol Distearate, Type I EP	55–66

#### Selection of the Synthesis Method

The development of a reproducible method for the synthesis of SLN-type lipid nanoparticles involved tests of their preparation by two methods:

- high-speed homogenization;
- high-pressure homogenization (HPH) at elevated temperatures.

As a result of the optimization of the synthesis method of lipid nanoparticles, involving the selection of the amount of lipid used (4.0 wt.%, 6.0 wt.%, and 8.0 wt.%), the amount of surfactant (0.5 wt.%, 1.5 wt.%, and 3.0 wt.%), the amount of active ingredient (1.0 wt.%, 2.0 wt.%, and 3.0 wt.%), and the pressure used in high-pressure hot homogenization (300 bar and 500 bar), the following SLN composition was selected: 2.0 wt.% of active ingredient (ethanol extract of *Ferula assa-foetida* L.), 6.0 wt.% of solid lipid (Witepsol®H15), and 1.5 wt.% of surfactant (Miranol Ultra).

In the following work, samples will be labeled as follows (Table 3): SLN—x wt.% Witepsol®H15, y wt.% Miranol Ultra, z wt.% extract, where: x is the weight percentage of lipid added, y is the weight percentage of surfactant added, and z is the weight percentage of *Ferula assa-foetida* L. extract added.

**Table 3.** Sample labeling mode for SLNs prepared by high-pressure homogenization.

Materials	Composition
SLN1	6.0 wt.% Witepsol®H15, 1.5 wt.% Miranol Ultra, without extract
SLN2	6.0 wt.% Witepsol®H15, 0.5 wt.% Miranol Ultra, 2.0 wt.% extract from <i>Ferula assa-foetida</i> L.
SLN4	6.0 wt.% Witepsol®H15, 1.5 wt.% Miranol Ultra, 2.0 wt.% extract from <i>Ferula assa-foetida</i> L.
SLN6	6.0 wt.% Witepsol®H15, 3.0 wt.% Miranol Ultra, 2.0 wt.% extract from <i>Ferula assa-foetida</i> L.
SLN9	6.0 wt.% Witepsol®H15, 1.5 wt.% Miranol Ultra, 1.0 wt.% extract from <i>Ferula assa-foetida</i> L.
SLN12	6.0 wt.% Witepsol®H15, 1.5 wt.% Miranol Ultra, 3.0 wt.% extract from <i>Ferula assa-foetida</i> L.
SLN13	4.0 wt.% Witepsol®H15, 0.5 wt.% Miranol Ultra, 1.0 wt.% extract from <i>Ferula assa-foetida</i> L.
SLN14	4.0 wt.% Witepsol®H15, 1.5 wt.% Miranol Ultra, 2.0 wt.% extract from <i>Ferula assa-foetida</i> L.
SLN15	8.0 wt.% Witepsol®H15, 1.5 wt.% Miranol Ultra, 2.0 wt.% extract from <i>Ferula assa-foetida</i> L.

#### Synthesis of SLN-Type Lipid Nanoparticles Using High-Speed Homogenization

Two phases were prepared: an aqueous phase, which was the surfactant Miranol Ultra and demineralized water, and a lipid phase, containing the lipid Witepsol®H15 and a plant extract. Both phases were heated to 42 °C, mixed, and then subjected to high-speed homogenization for 110 s. Homogenization was carried out at 24,000 rpm using an Ultra-Turrax®DI25 homogenizer (IKA WERKE GmbH, Staufen im Breisgau, Germany). The samples obtained during these experiments were labeled SLN1/HS and SLN4/HS for the systems without and with plant extract (2 wt.%), respectively.

#### Synthesis of SLN-Type Lipid Nanoparticles Using HPH

Two phases were prepared: an aqueous phase, which was the surfactant Miranol Ultra and demineralized water, and a lipid phase, containing the lipid Witepsol®H15 and a plant extract. All ingredients were weighed in amounts enabling the preparation of 50 g of the emulsion. Both phases were heated to 42 °C, mixed, and then subjected to high-speed pre-homogenization at 10,000 rpm for 20 s using an Ultra-Turrax®DI25 homogenizer. The resulting pre-emulsion was then subjected to a hot high-pressure homogenization using a Panda Plus 2000 homogenizer (GEA, Dusseldorf, Germany). The homogenization pressure

was 300 or 500 bar, and, after reaching the set pressure value, the sample was homogenized in cycles for 90 s.

#### 2.2.4. Physicochemical Characteristics of the Obtained SLNs

##### Average Particle Size and Polydispersity Index

Average particle size Z-average (Z-Ave) and polydispersity index (PDI) were determined using the Dynamic Light Scattering (DLS) method.

Each sample was tested using a Litesizer 500 particle size analyzer (Anton Paar GmbH, Austria) at 25 °C. Before analysis, the as-obtained SLN dispersions were diluted 500-fold in highly demineralized water (Milli-Q®Plus, Millipore, Germany), then the prepared sample was placed in a measuring cell made of polystyrene, which was filled to a height of about 10 mm. During one measurement cycle, three measurements were taken for each Z-Ave value. After the measurements were completed, the arithmetic mean and standard deviation of the results were calculated.

##### Zeta Potential (ZP)

Zeta potential (ZP) was tested using a Zetasizer Nano Z instrument (Malvern Instruments, Worcestershire, UK). Each SLN dispersion was diluted 500-fold with highly demineralized water (Milli-Q®Plus). A minimum of 1 cm<sup>3</sup> of the prepared sample was then transferred using a syringe into a U-shaped capillary (DTS1060), which, after sealing, was placed in the instrument's measuring chamber. The ZP value was measured three times per cycle and then calculated by the system software using the Helmholtz–Smoluchowski equation. After the measurements were completed, the arithmetic mean and standard deviation of the results were calculated.

##### X-ray Diffraction (XRD)

The degree of crystallinity and the presence of polymorphic forms of the lipid matrix of the obtained lipid nanoparticles were determined by X-ray diffraction (XRD) analysis. XRD patterns were obtained using a D8 Advance powder diffractometer with a Johansson monochromator (Bruker, Billerica, MA, USA;  $\lambda$  Cu-K $\alpha$  = 0.15406 nm). Sample preparation consisted of placing the tested dispersions of lipid nanoparticles on a Petri dish and drying them at room temperature. The obtained samples were analyzed in the following ranges: small angles (SAXD: 0.6–0.8°) at a scanning speed of 0.02°/3 s and wide angles (WAXD: 6–60°) at a scanning speed of 0.05°/1 s.

##### Differential Scanning Calorimetry (DSC)

The polymorphic forms of the lipid matrix of the lipid nanoparticles were evaluated based on the results of the thermal analysis performed with a DSC 8500 differential scanning calorimeter (Perkin Elmer, Waltham, MA, USA). The instrument was calibrated prior to the measurements. During the measurements, the aluminum plate was filled with a sample of lipid or a sample of the solid dispersion of lipid nanoparticles under study. The sample was then gradually heated from 25 °C to 300 °C in a flow of nitrogen (20 cm<sup>3</sup>/min) at a rate of 5 °C per minute. After reaching the desired temperature, the sample was kept at 300 °C for 1 min, and then cooled to –20 °C with the above parameters.

#### 2.2.5. Quantitative Determination of Ferulic Acid Present in the Ethanol Extract from *Ferula assa-foetida* L. and in Solid Lipid Nanoparticles Incorporated with This Extract

Quantitative determination of the ferulic acid present in the ethanol extract from *Ferula assa-foetida* L. and in the solid lipid nanoparticles incorporated with the above-mentioned extract was performed using a Varian 920-LC high-performance liquid chromatograph (Agilent Technologies, Stevens Creek Blvd.; Santa Clara, CA, USA) equipped with an automatic sample changer. The chromatographic determination of ferulic acid involved the appropriate preparation of samples of solid lipid nanoparticles containing the active substance to be determined (ferulic acid). The analysis process consisted of the following steps:

- Preparation of standard solutions for the calibration curve. The first step of the work was to prepare a methanolic stock solution of ferulic acid at a concentration of 0.260 mg/cm<sup>3</sup>. Ferulic acid standard solutions of 0.013, 0.026, 0.065, and 0.130 mg/cm<sup>3</sup> were then prepared from the stock solution by successive dilutions.
- Preparation of ethanol extract from *Ferula assa-foetida* L. and SLN incorporated with the above-mentioned extract for chromatographic analysis. The *Ferula assa-foetida* L. extract obtained according to the procedure described in Section 2.2.1 was diluted 100 times with methanol. The resulting solution was filtered through a syringe PTFE filter with a pore diameter of 0.45 µm and 1.5 cm<sup>3</sup> was transferred to a glass vial for HPLC analysis. At the same time, SLN samples incorporated with *Ferula assa-foetida* L. extract were subjected to the extraction process, which was carried out as follows: 1.0 g of sample was poured into 1.0 g of methanol, then the process was carried out for 2 h, with the first 0.5 h including treatment of the sample in the ultrasonic bath. Then the sample was transferred to a magnetic stirrer and stirred for 1 h and again treated in the ultrasonic bath for 0.5 h.
- Chromatographic analysis. Chromatographic analysis was performed according to the conditions given in Table 4. Each of the tested samples was subjected to two measurements, and the arithmetic mean was calculated from the obtained results.

**Table 4.** Chromatographic analysis conditions.

Column	Microsorb-MV 100 C8 250 × 4.6 mm (5 µm)
Mobile phase	Methanol/1% CH <sub>3</sub> COOH (70/30 v/v)
The flow rate of the mobile phase [cm <sup>3</sup> /min]	1
The volume of samples dispensed [µL]	5
Detector	UV-Vis
Analytical wavelength [nm]	319
Total analysis time [min]	20

### 3. Results and Discussion

#### 3.1. GC-MS Analysis of Ethanol Extract from *Ferula assa-foetida* L.

The resulting plant extract was analyzed using gas chromatography coupled to a mass detector. In this extract, ferulic acid was identified as the main component (Figures 3 and 4). MS spectra (Figure 4) show  $m/z$  values confirming the presence of ferulic acid in the extract, alongside other fragments:  $m/z = 194$  (molecular ion),  $m/z = 179$  -ion formed by loss of [CH<sub>3</sub>] from the methoxy group,  $m/z = 150$  -ion from carboxyl group elimination,  $m/z = 133$  -ion created by simultaneous loss of the carboxyl group and [CH<sub>3</sub>] from the methoxy group,  $m/z = 77$  -[C<sub>6</sub>H<sub>5</sub>]<sup>+</sup> fragment formed from the aromatic ring.

The obtained spectra confirmed that the proposed extraction procedure allows extracts containing ferulic acid to be obtained. Moreover, *Ferula assa-foetida* L. has the potential to be a natural source for this compound in cosmetic applications, since ferulic acid exhibits anti-aging and depigmentation properties, as well as prevents the formation of sun discoloration [29,30].

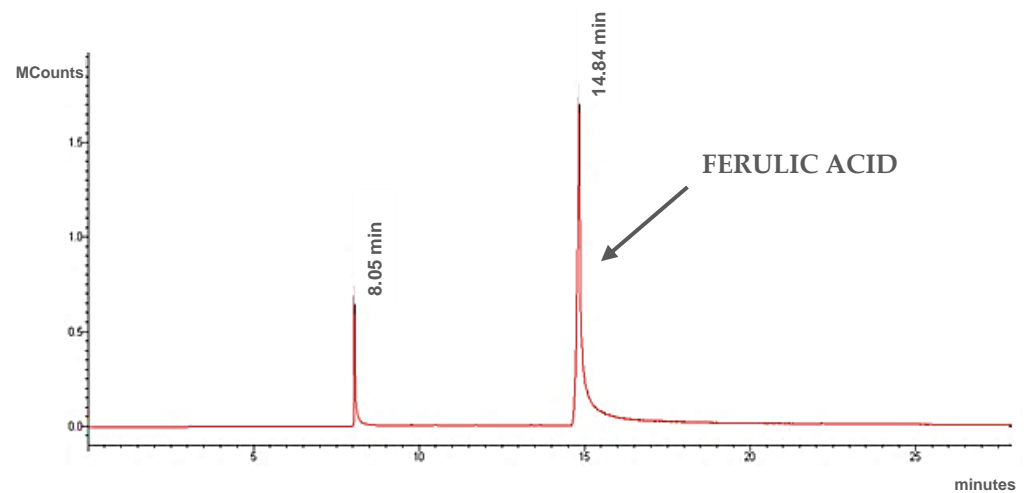


**Figure 3.** Chromatogram of ethanol extract of *Ferula assa-foetida* L.

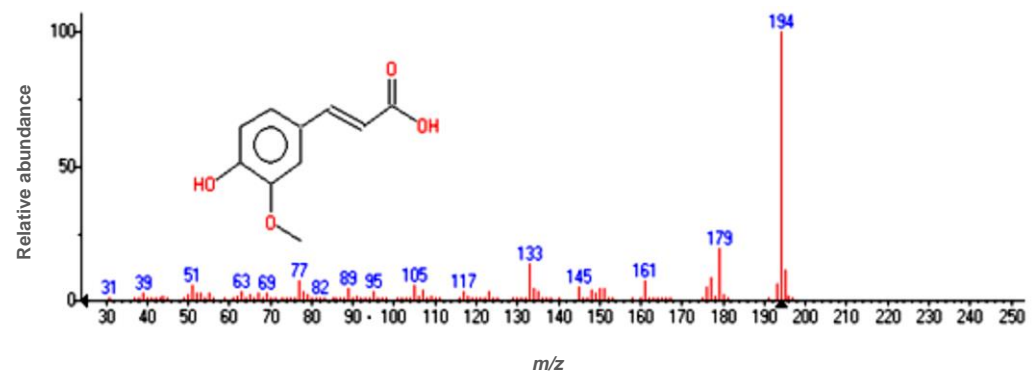


**Figure 4.** Mass spectrum of ferulic acid at a retention time of 14.84 min.

### 3.2. Optimization of the Synthesis of Solid Lipid Nanoparticles

To optimize the parameters for the synthesis of lipid nanoparticles incorporated with ethanol extract from *Ferula assa-foetida* L., the following were varied:

- the method for their preparation (high-speed homogenization; high-pressure hot (HPH) homogenization);
- the pressure used in the HPH-based method (300 bar and 500 bar);
- the amount of lipid used (4.0 wt.%, 6.0 wt.%, and 8.0 wt.%);
- the amount of surfactant used (0.5 wt.%, 1.5 wt.%, and 3.0 wt.%);
- the amount of *Ferula assa-foetida* L. extract added (1.0 wt.%, 2.0 wt.%, and 3.0 wt.%).

Based on the evaluation of average particle size (Z-Ave), measurement of zeta potential (ZP), and polydispersity index (PDI) given in Table 5, the optimized parameters for SLN synthesis were selected. It should be noted that Table 5 does not include the results for solid lipid nanoparticles obtained at a pressure of 300 bar because these dispersions delaminated immediately after synthesis.

**Table 5.** Optimization of SLN synthesis parameters—comparison of zeta potential (ZP), polydispersity index (PDI), and average particle size (Z-Ave) of solid lipid nanoparticles (SLN) measured on the day of synthesis, and on the 7th, and 28th day after synthesis.

Sample Name	Day	ZP [mV] ± SD	PDI [-] ± SD	Z-Ave [nm] ± SD
HPH, 500 bar, 4.0 wt.% Witepsol®H15, 0.5 wt.% Miranol Ultra				
SLN without extract	0	−45.63 ± 0.78	0.12 ± 0.01	162 ± 1.8
	7	−29.36 ± 0.35	0.18 ± 0.01	160 ± 2.9
	28	−42.60 ± 0.46	0.18 ± 0.01	164 ± 0.7
SLN13 1.0 wt.% <i>Ferula assa-foetida</i> L. extract	0	−38.63 ± 0.51	0.16 ± 0.00	147 ± 1.3
	7	−30.80 ± 0.65	0.15 ± 0.00	147 ± 2.1
	28	−37.82 ± 0.46	0.18 ± 0.00	150 ± 0.9
HPH, 500 bar, 4.0 wt.% Witepsol®H15, 1.5 wt.% Miranol Ultra				
SLN without extract	0	−43.03 ± 0.98	0.20 ± 0.02	170 ± 1.2
	7	−46.67 ± 1.37	0.21 ± 0.01	177 ± 0.7
	28	−42.93 ± 0.61	0.21 ± 0.01	171 ± 2.2
SLN14 2.0 wt.% <i>Ferula assa-foetida</i> L. extract	0	−39.93 ± 0.06	0.18 ± 0.01	159 ± 0.6
	7	−40.57 ± 0.51	0.19 ± 0.01	161 ± 0.2
	28	−49.07 ± 4.20	0.30 ± 0.02	189 ± 4.5
HPH, 500 bar, 6.0 wt.% Witepsol®H15, 0.5 wt.% Miranol Ultra				
SLN without extract	0	−31.53 ± 0.58	0.22 ± 0.01	196 ± 2.0
	7	−34.20 ± 1.65	0.21 ± 0.02	173 ± 0.5
	28	−34.00 ± 0.90	0.20 ± 0.01	173 ± 1.8
SLN2 2.0 wt.% <i>Ferula assa-foetida</i> L. extract	0	−25.30 ± 0.98	0.27 ± 0.01	205 ± 2.8
	7	−38.73 ± 1.90	0.26 ± 0.00	205 ± 2.0
	28	−42.30 ± 0.60	0.24 ± 0.01	204 ± 2.8
HPH, 500 bar, 6.0 wt.% Witepsol®H15, 1.5 wt.% Miranol Ultra				
SLN1 without extract	0	−45.63 ± 0.78	0.17 ± 0.01	163 ± 1.8
	7	−29.36 ± 0.35	0.18 ± 0.01	160 ± 2.9
	28	−42.60 ± 0.88	0.18 ± 0.01	164 ± 0.8
	3 months	−41.97 ± 0.47	0.16 ± 0.01	163 ± 1.1
SLN4 2.0 wt.% <i>Ferula assa-foetida</i> L. extract	0	−38.63 ± 0.51	0.16 ± 0.01	148 ± 1.3
	7	−30.80 ± 0.65	0.15 ± 0.00	147 ± 2.1
	28	−37.58 ± 0.73	0.17 ± 0.01	151 ± 0.9
	3 months	−35.70 ± 0.95	0.15 ± 0.01	147 ± 0.9
SLN9 1.0 wt.% <i>Ferula assa-foetida</i> L. extract	0	−35.23 ± 1.03	0.29 ± 0.02	206 ± 0.6
	7	−39.63 ± 0.68	0.24 ± 0.01	192 ± 1.7
	28	−40.60 ± 0.90	0.23 ± 0.02	192 ± 0.2
SLN12 3.0 wt.% <i>Ferula assa-foetida</i> L. extract	0	−25.70 ± 0.89	0.16 ± 0.00	153 ± 3.6
	7	−33.87 ± 0.76	0.16 ± 0.00	154 ± 1.8
	28	−38.00 ± 1.12	0.16 ± 0.01	155 ± 1.1

Table 5. Cont.

Sample Name	Day	ZP [mV] ± SD	PDI [-] ± SD	Z-Ave [nm] ± SD
HPH, 500 bar, 6.0 wt.% Witepsol <sup>®</sup> H15, 3.0 wt.% Miranol Ultra				
SLN without extract	0	−33.40 ± 0.52	0.21 ± 0.01	173 ± 1.8
	7	−44.37 ± 0.32	0.21 ± 0.02	185 ± 2.3
	28	−47.10 ± 2.22	0.21 ± 0.02	175 ± 0.8
SLN6 2.0 wt.% <i>Ferula assa-foetida</i> L. extract	0	−37.70 ± 1.31	0.23 ± 0.01	177 ± 1.3
	7	−43.67 ± 0.32	0.26 ± 0.01	179 ± 4.2
	28	−41.90 ± 0.74	0.22 ± 0.01	181 ± 2.8
HPH, 500 bar, 8.0 wt.% Witepsol <sup>®</sup> H15, 1.5 wt.% Miranol Ultra				
SLN without extract	0	−49.10 ± 0.36	0.56 ± 0.02	311 ± 4.5
	7	−49.95 ± 1.14	0.85 ± 0.02	397 ± 8.2
	28	−48.93 ± 0.46	0.53 ± 0.02	301 ± 4.2
SLN15 2.0 wt.% <i>Ferula assa-foetida</i> L.	0	−40.20 ± 0.26	0.19 ± 0.01	170 ± 0.4
	7	−41.77 ± 1.10	0.18 ± 0.02	175 ± 0.6
	28	−43.00 ± 0.70	0.20 ± 0.00	169 ± 1.0
HIGH-SPEED HOMOGENIZATION 6.0 wt.% Witepsol <sup>®</sup> H15, 1.5 wt.% Miranol Ultra, 110s Ultra, 24 000 rpm				
SLN1/HS without extract	0	−63.43 ± 3.48	1.00 ± 0.00	4397 ± 874
	7	−55.50 ± 0.93	0.57 ± 0.03	6527 ± 441
	28	delamination	delamination	delamination
SLN4/HS 2.0 wt.% <i>Ferula assa-foetida</i> L. extract	0	−50.03 ± 1.07	0.39 ± 0.17	5913 ± 251
	7	delamination	delamination	delamination
	28	delamination	delamination	delamination

For stable emulsions, the PDI coefficient should be <0.30 [31]. The PDI coefficient indicates the degree of dispersibility, i.e., the statistical dispersion of the particle mass [32]. It is important to achieve the lowest possible PDI values (<0.30 [-]), which at the same time confirms the stability of the tested formulation [33]. During our study, we aimed to obtain the smallest possible Z-Ave values that could be gained using the synthesis parameters we chose. It was also important to obtain a dispersion with the narrowest possible particle size distribution (expressed as a PDI coefficient) so that the dispersion would be stable during long-term storage. Dispersions with a narrow particle size distribution do not tend to experience sintering of the particles, and thus the Z-Ave and PDI parameters can be used to evaluate the stability of the obtained SLNs. The lowest PDI values were obtained for samples synthesized as follows: HPH, 500 bar, 4.0 wt.% lipid, 0.5 wt.% surfactant, and 1.0 wt.% extract (SLN13), and HPH, 500 bar, 6.0 wt.% lipid, 1.5 wt.% surfactant, and 2.0 wt.% *Ferula assa-foetida* L. extract (SLN4) (Table 5). This indicates the highest stability of these samples. In addition, the stabilizing effect of the introduced plant extract can also be noted—comparing the PDI value for the aforementioned SLN13 and SLN4 samples and their counterparts containing no extract, it can be noted that, after an analogous period of time (28 days), the PDI changes more distinctly for SLNs containing no plant extract, increasing from 0.12 ± 0.01 to 0.18 ± 0.01 in the case of “empty” SLN and from 0.16 ± 0.01 to 0.17 ± 0.01 and 0.18 ± 0.01 for SLN4 and SLN13, respectively.

It is also worth mentioning that the as-synthesized SLN samples differ significantly in terms of the PDI coefficient, which clearly depends on the proportion of components used in the HPH process. Comparing the PDI values (Table 5) for the SLN samples, it can be seen that they vary from 0.56 ± 0.02 [-] for SLN prepared in the system of 8.0 wt.% Witepsol<sup>®</sup>H15

and 1.5 wt.% Miranol Ultra, through  $0.20 \pm 0.02$  [-] for SLNs synthesized with 4.0 wt.% Witepsol®H15 and 1.5 wt.% Miranol Ultra, down to the lowest values of  $0.12 \pm 0.01$  for the substrate ratio of 6.0 wt.% Witepsol®H15 and 1.5 wt.% Miranol Ultra. It was the latter SLNs that were selected for further study, as the PDI values, as well as the ZP, suggested that they would be the most stable during storage.

In addition, to determine the potential stability of the obtained lipid nanoparticles, the zeta potential (ZP) was also measured. ZP is one of the key parameters describing the process of particle behavior in suspension and is used to analyze the electrostatic properties of suspensions [34]. It is assumed that the tested material can be considered stable if the absolute value of the zeta potential is greater than  $-30$  mV [35,36]. The lowest absolute ZP values ( $-25.30$  mV  $\pm$  0.98 mV) were obtained for sample SLN4 obtained by HPH, 500 bar, 6.0 wt.% lipid, 0.5 wt.% surfactant, and 2.0 wt.% *Ferula assa-foetida* L. extract, while the highest absolute values were recorded for sample SLN1/HSH obtained by high-speed homogenization ( $-63.43$  mV  $\pm$  3.48 mV). However, for samples obtained by this method, the other parameters (PDI, Z-Ave) deviate significantly from acceptable values. In addition, both the SLN1/HSH and SLN4/HSH samples obtained by only high-speed homogenization delaminated within 28 days of the day of synthesis.

In summary, the most efficient method for synthesizing lipid nanoparticles (observations based on the data in Table 5), is the high-pressure homogenization (HPH) method and a system containing 6.0 wt.% Witepsol®H15 lipid, 1.5 wt.% surfactant, and 2.0 wt.% *Ferula assa-foetida* L. extract.

### 3.3. Characterization of the Lipid Matrix in Synthesized SLN-Type Lipid Nanoparticles

Characterization of the lipid matrix in SLN-type lipid nanoparticles was performed using X-ray diffraction (XRD) and differential scanning calorimetry (DSC). The obtained results are presented in Figures 5 and 6, respectively.

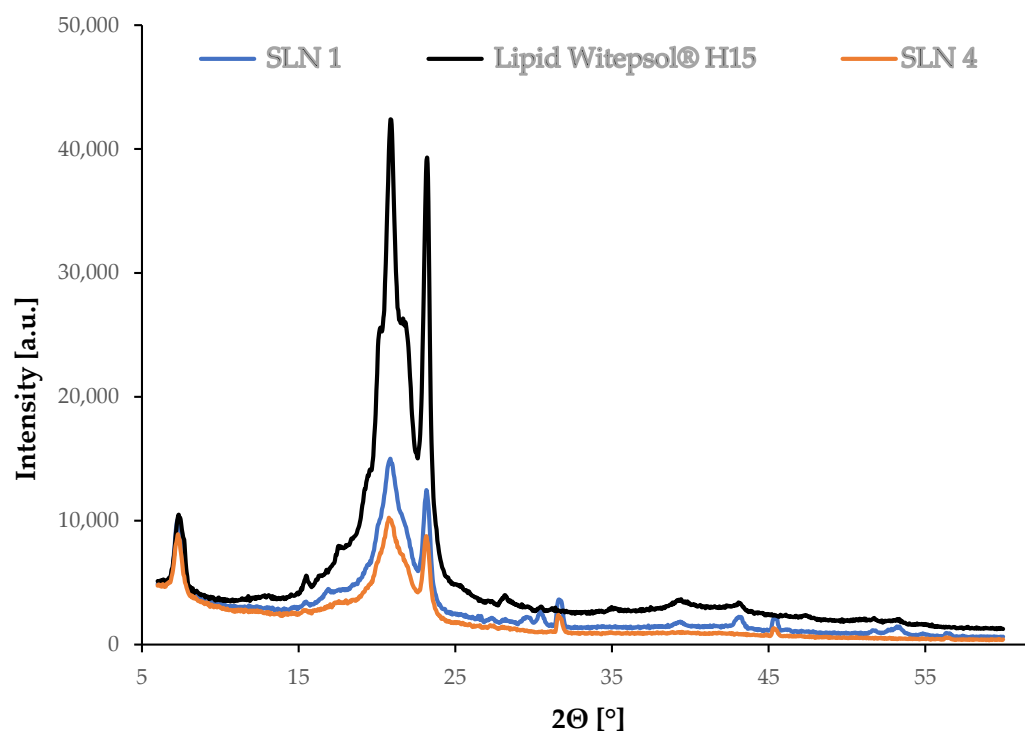


**Figure 5.** Diffractograms for synthesized SLNs: “empty” (without extract, SLN1), incorporated with *Ferula assa-foetida* L. extract (SLN4) and Witepsol®H15 lipid.

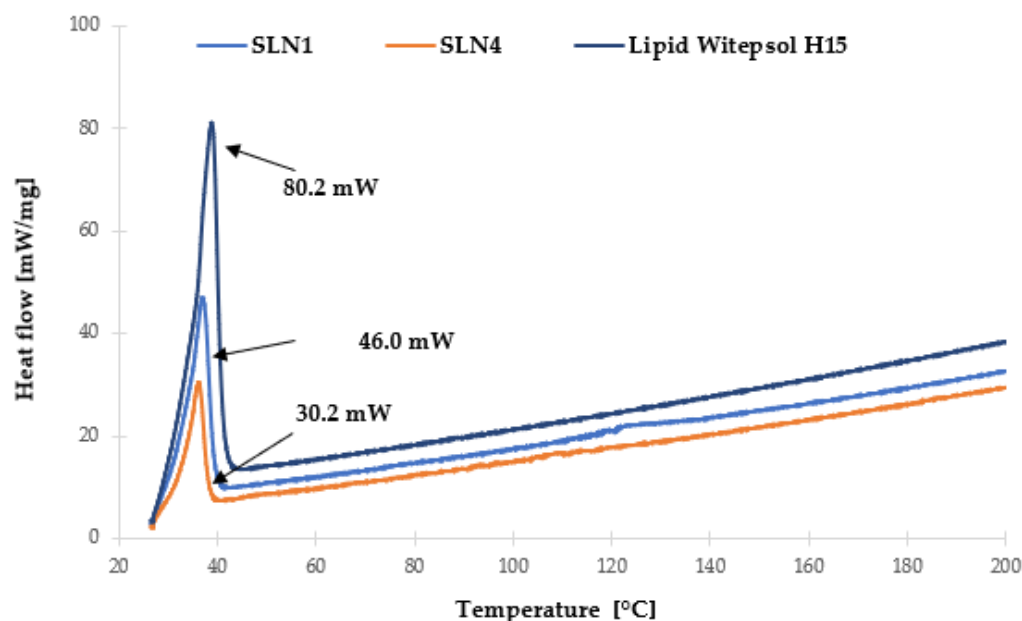


**Figure 6.** Comparison of DSC thermograms recorded during heating from 25 to 200 °C of synthesized SLNs and Witepsol<sup>®</sup>H15 lipid.

Figure 5 shows a summary of the diffractograms of the lipid and the tested SLN-type lipid nanoparticles, “empty”, meaning without incorporated extract (SLN1), and incorporated with *Ferula assa-foetida* L. extract (SLN4). XRD measurements enable the determination of the possible changes in the crystallinity of the components that may occur during hot high-pressure homogenization. The polymorphic structure has a direct influence on the encapsulation efficiency and exclusion of the active substance during SLN storage [37]. On the basis of the XRD measurements, a comparison of the polymorphic structure was made between the obtained SLNs and the solid lipid, which was the reference sample.

Characteristic reflections were observed at  $2\theta = 20.86^\circ$  and  $23.15^\circ$  on the diffractogram of the Witepsol<sup>®</sup>H15 solid lipid (Figure 5). The occurrence of these signals was also noted on the diffractograms of the tested lipid nanoparticles, confirming the presence of the most stable  $\beta$  form and the  $\beta'$  polymorphic variation (a metastable form, possessing disordered regions and a partially amorphous state). This is characteristic of triacylglycerol-based lipids that occur in the colloidal state [38]. In the case of the solid lipid nanoparticles, both the “empty” (SLN1) sample and the sample incorporated with *Ferula assa-foetida* L. ethanol extract (SLN4) showed reduced peak intensity, indicating some disruptions in the Witepsol<sup>®</sup>H15 polymorphic forms induced during SLN synthesis [39].

In addition, the characterization of the lipid matrix was carried out using DSC analysis (Figure 6), based on which, the determination of the polymorphic variety of a particular lipid used in the synthesis of lipid nanoparticles was performed. This analysis is based on the assumption that different polymorphic varieties of lipids have different melting points and corresponding enthalpies [40].

Witepsol<sup>®</sup>H15, which is a mixture of triacylglycerols of saturated fatty acids with the addition of mono- and diacylglycerols, in the solid state, is predominantly in the stable  $\beta$ -form, appearing on the thermogram as a single exothermic peak at 38.81 °C (process intensity 80.2 mW). The transition of solid lipid into a colloidal state, associated with the formation of a lipid nanoparticle, caused a decrease in the melting temperature of the lipid nanoparticle dispersion under study. For “empty” SLN-type lipid nanoparticles (SLN1), a single exothermic peak was also observed at 37.48 °C (46.0 mW). For SLN incorporated with *Ferula assa-foetida* L. extract (SLN4), an exothermic peak was observed at 36.97 °C (30.2 mW). The recorded changes of this parameter were determined to be the result of partial transformation of the  $\beta$  form into the  $\beta'$  form—characteristic of mixtures of

triacylglycerols in the colloidal state [41]. This is also in good agreement with the results obtained during the XRD measurements. In addition, after analyzing the obtained results, it was found that the presence of *Ferula assa-foetida* L. extract in the lipid matrix of SLNs required a lower melting temperature for the mixture of triacylglycerols of saturated fatty acids with the addition of mono- and di-acylglycerols compared to the sample without the incorporated active ingredient [39]. Moreover, the minimal shift in the thermograms of the solid lipid nanoparticle samples, namely, “empty” (SLN1,) as well as those incorporated with *Ferula assa-foetida* L. extract (SLN4), may be due to the existence of a molecularly dispersed active ingredient (ferulic acid) in the lipid matrix [42].

### 3.4. Quantitative Determination of Ferulic Acid Present in the Ethanol Extract from *Ferula assa-foetida* L. and in Solid Lipid Nanoparticles Incorporated with This Extract

Based on the chromatograms of a ferulic acid standard, the retention time was determined and found to be 3.26 min. The content of ferulic acid in the samples tested was calculated based on the calibration curve equation:  $y = 427.28x - 0.7356$  ( $R^2 = 0.998$ ). The calibration curve was prepared according to the analysis of the series of solutions prepared as described in Section 2.2.5. The results obtained from the HPLC analysis are summarized in Table 6.

**Table 6.** Ferulic acid concentration evaluated on the basis of HPLC analysis.

Sample	Sample Composition	Ferulic Acid Content [mg/cm <sup>3</sup> ]
SLN1	S: 1.5%; E: 0.0%; L: 6.0%	0.00
SLN2	S: 0.5%; E: 2.0%; L: 6.0%	0.11
SLN4	S: 1.5%; E: 2.0%; L: 6.0%	0.05
SLN6	S: 3.0%; E: 2.0%; L: 6.0%	0.07
SLN9	S: 1.5%; E: 1.0%; L: 6.0%	0.04
SLN12	S: 1.5%; E: 3.0%; L: 6.0%	0.15
Extract from <i>Ferula assa-foetida</i> L.	—	18.87

where: S—surfactant, E—extract, L—lipid.

In the *Ferula assa-foetida* L. extract, the amount of ferulic acid is 18.87 mg/cm<sup>3</sup>. In contrast, in the case of the SLN4 sample, the composition of which after optimization was indicated to be the most suitable, the content is 0.05 mg/cm<sup>3</sup> (it should be remembered that a maximum of 3 wt.% of the extract was used, which corresponds to 0.56 mg/cm<sup>3</sup> of ferulic acid). The amount of *Ferula assa-foetida* L. extract added during the SLN synthesis affects the final ferulic acid content of the sample—for SLN12, 0.15 mg/cm<sup>3</sup> of ferulic acid was recorded, meaning that the maximum loading of ferulic acid can be estimated as ~27%.

Our studies on polydispersity index (PDI), zeta potential (ZP), and average particle size (Z-Ave) showed that the most optimal chemical composition for the studied SLNs is the system of 1.5% of surfactant, 6.0% of lipid, and 2% of plant extract, as the PDI value of 0.15, ZP of −37.82 mV, and Z-Ave of 150.00 nm on the 28th day after synthesis were obtained for this system. However, the highest level of extract loading, i.e., the highest ferulic acid content, was obtained for SLNs prepared with 1.5% surfactant, 6.0% lipid, and 3% extract. It is worth noting that these SLNs were also characterized by satisfactory values of PDI, ZP, and Z-Ave values (0.16, −33.87, and 153.70, respectively). Therefore, it can be assumed that this type of system carries the highest potential to be used as a carrier of ferulic acid in cosmetic products.

Moreover, the conducted chromatographic analyses allowed us to conclude that the quantity of introduced ferulic acid varies not only with the amount of *Ferula assa-foetida* L. extract used but also with the composition of the SLN.

#### 4. Conclusions

The results show that the most efficient procedure for synthesizing lipid nanoparticles is the high-pressure homogenization (HPH) method operating at 500 bar, applied to a system containing 6.0 wt.% of Witepsol<sup>®</sup>H15 lipid, 1.5 wt.% of surfactant Miranol Ultra, and 2.0 wt.% of *Ferula assa-foetida* L. extract. This was confirmed by measurements made three months after SLN synthesis, which showed that the mean particle size did not change, while the ZP value decreased slightly but it was still at a level typical for stable nanoparticles. The incorporation of plant extracts into lipid nanoparticles reduces the particle size but it does not influence significantly the stability, as shown by the values of PDI and ZP. These parameters were also maintained during measurements performed three months after the synthesis of SLNs incorporated with the plant extract.

The incorporation of *Ferula assa-foetida* L.–ethanol extract into SLNs was successfully performed, which was confirmed by HPLC analysis. Experiments showed that it was possible to achieve an encapsulation efficiency of ferulic acid as high as 27%.

Our study shows that SLNs incorporated with the *Ferula assa-foetida* L. extract may be applied as a potential delivery platform for ferulic acid in cosmetic products. Nevertheless, some additional tests are still required.

**Author Contributions:** Conceptualization, A.F.-G. and I.N.; methodology, S.L., A.W. and A.F.-G.; investigation, S.L., A.W. and A.F.-G.; data curation, S.L., A.W. and A.F.-G.; writing—original draft preparation, S.L., A.W. and A.F.-G.; writing—review and editing, I.N.; visualization, S.L., A.W. and A.F.-G.; supervision, A.W. and A.F.-G. All authors have read and agreed to the published version of the manuscript.

**Funding:** This research received no external funding.

**Institutional Review Board Statement:** Not applicable.

**Informed Consent Statement:** Not applicable.

**Data Availability Statement:** Not applicable.

**Acknowledgments:** hab. Anna Kotłowska from the Faculty of History at Adam Mickiewicz University, Poznań, is kindly acknowledged for her help with reviewing historical databases.

**Conflicts of Interest:** The authors declare no conflict of interest.

#### References

1. Banach, A. *Historia Pięknej Kobiety (History of a Beautiful Woman)*; Wydawnictwo Literackie: Warszawa, Poland, 1991.
2. Golińska, D. *Kanony Kobiecej Urody. Od Starożytnego Egiptu po XXI Wiek (Canons of Female Beauty. From Ancient Egypt to the 21st Century)*; Wydawnictwo Buchmann: Warszawa, Poland, 2014.
3. Posz, E. Znaczenie roślin kosmetycznych w utrzymaniu higieny w kulturach starożytnych. In *Czystość i Brud. Higiena w Starożytności (Cleanliness and Dirt. Hygiene in Antiquity)*, 1st ed.; Korpalska, W., Ślusarczyk, W., Eds.; Wydawnictwo Naukowe Uniwersytetu Mikołaja Kopernika: Toruń, Poland, 2013; pp. 279–294.
4. Łuczak, K. *Silphium z Cyrene. Skarb antycznej medycyny (Silphium of Cyrene. A treasure of ancient medicine)*. *Kwart. Hist. Kult. Mater.* **2015**, *63*, 3–14.
5. Kotłowska, A. Silfion—Dawne bogactwo Cyrenejki (Silfion—The former wealth of Cyrenaica). *Meander* **2003**, *58*, 409–416.
6. Hlasiwetz, H.; Barth, L. Mittheilungen aus dem chemischen Laboratorium in Innsbruck I, Ueber einige Harze [Zersetzungsproducte derselben durch schmelzendes Kali]. *Justus Liebigs Ann. Chem.* **1866**, *138*, 61–76. [[CrossRef](#)]
7. Dutt, S. General synthesis of  $\alpha$ -unsaturated acids from malonic acid. *QJ Chem. Soc.* **1925**, *1*, 297–301.
8. Stuper-Szablewska, K.; Przybylska, A.; Kurasiak-Popowska, D.; Perkowski, J. Ferulic acid: Properties, determination, and application in cosmetic industry. *Przem. Chem.* **2017**, *96*, 2070–2076. [[CrossRef](#)]
9. Park, H.-J.; Cho, J.-H.; Hong, S.-H.; Kim, D.-H.; Jung, H.-Y.; Kang, I.-K.; Cho, Y.-J. Whitening and anti-wrinkle activities of ferulic acid isolated from *Tetragonia tetragonioides* in B16F10 melanoma and CCD-986sk fibroblast cells. *J. Nat. Med.* **2018**, *72*, 127–135. [[CrossRef](#)]
10. Nile, S.H.; Ko, E.Y.; Kim, D.H.; Keum, Y.S. Screening of ferulic acid-related compounds as inhibitors of xanthine oxidase and cyclooxygenase-2 with anti-inflammatory activity. *Rev. Bras. Farmacogn.* **2016**, *26*, 50–55. [[CrossRef](#)]
11. Londoño, C.A.; Rojas, J.; Yarcce, C.J.; Salamanca, C.H. Design of Prototype Formulations for *In Vitro* Dermal Delivery of the Natural Antioxidant Ferulic Acid Based on Ethosomal Colloidal Systems. *Cosmetics* **2019**, *6*, 5. [[CrossRef](#)]

12. Lin, F.-H.; Lin, J.-Y.; Gupta, R.D.; Tournas, J.A.; Burch, J.A.; Selim, M.A.; Monteiro-Riviere, N.A.; Grichnik, J.M.; Zielinski, J.; Pinnell, S.R. Ferulic Acid Stabilizes a Solution of Vitamins C and E and Doubles its Photoprotection of Skin. *J. Investig. Dermatol.* **2005**, *125*, 826–832. [[CrossRef](#)]
13. Farzaneh, S.K.; Es-Haghi, A.; Tabrizi, M.H.; Shabestarian, H. The loaded *Ferula assa-foetida* seed essential oil in Solid lipid nanoparticles (FSEO-SLN) as the strong apoptosis inducer agents in human NTERA-2 embryocarcinoma cells. *Mater. Technol.* **2022**, *37*, 1120–1128. [[CrossRef](#)]
14. Kumar, N.; Pruthi, V. Potential applications of ferulic acid from natural sources. *Biotechnol. Rep.* **2014**, *4*, 86–93. [[CrossRef](#)]
15. Farooq, S.; Mir, S.A.; Shah, M.A.; Manickavasagan, A. Extraction techniques (Chapter 2). In *Plant Extracts: Applications in the Food Industry*; Mir, S.A., Shah, M.A., Manickavasagan, A., Eds.; Academic Press: London, UK, 2022; pp. 23–37. [[CrossRef](#)]
16. Paliwal, R.; Paliwal, S.R.; Kenwat, R.; Kurmi, B.D.; Sahu, M.K. Solid lipid nanoparticles: A review on recent perspectives and patents. *Expert Opin. Ther. Pat.* **2020**, *30*, 179–194. [[CrossRef](#)]
17. Khater, D.; Nsairat, H.; Odeh, F.; Saleh, M.; Jaber, A.; Alshaer, W.; Al Bawab, A.; Mubarak, M.S. Design, Preparation, and Characterization of Effective Dermal and Transdermal Lipid Nanoparticles: A Review. *Cosmetics* **2021**, *8*, 39. [[CrossRef](#)]
18. Borges, A.; de Freitas, V.; Mateus, N.; Fernandes, I.; Oliveira, J. Solid Lipid Nanoparticles as Carriers of Natural Phenolic Compounds. *Antioxidants* **2020**, *9*, 998. [[CrossRef](#)]
19. Musielak, E.; Feliczak-Guzik, A.; Nowak, I. Synthesis and Potential Applications of Lipid Nanoparticles in Medicine. *Materials* **2022**, *15*, 682. [[CrossRef](#)]
20. Musielak, E.; Feliczak-Guzik, A.; Nowak, I. Optimization of the Conditions of Solid Lipid Nanoparticles (SLN) Synthesis. *Molecules* **2022**, *27*, 2202. [[CrossRef](#)] [[PubMed](#)]
21. Gasco, M.R. Method for Producing Solid Lipid Microspheres Having a Narrow Size Distribution. U.S. Patent US5250236A, 5 October 1993.
22. Souto, E.B.; Almeida, A.J.; Müller, R.H. Lipid Nanoparticles (SLN<sup>®</sup>, NLC<sup>®</sup>) for Cutaneous Drug Delivery: Structure, Protection and Skin Effects. *J. Biomed. Nanotech.* **2007**, *3*, 317–331. [[CrossRef](#)]
23. Lucks, S.; Muller, R. Arzneistoffträger aus Festen Lipidteilchen (Feste Lipidnanosphären (sln)). German Patent EP0605497B2, 18 September 1991.
24. Kalaycioglu, G.D.; Aydogan, N. Preparation and investigation of solid lipid nanoparticles for drug delivery. *Colloids Surf. A* **2016**, *510*, 77–86. [[CrossRef](#)]
25. Souto, E.B.; Doktorovova, S.; Gonzalez-Mira, E.; Egea, M.A.; Garcia, M.L. Feasibility of lipid nanoparticles for ocular delivery of anti-inflammatory drugs. *Curr. Eye Res.* **2010**, *35*, 537–552. [[CrossRef](#)]
26. Khairnar, S.V.; Pagare, P.; Thakre, A.; Nambiar, A.R.; Junnuthula, V.; Abraham, M.C.; Kolimi, P.; Nyavanandi, D.; Dyawanapelly, S. Review on the Scale-Up Methods for the Preparation of Solid Lipid Nanoparticles. *Pharmaceutics* **2022**, *14*, 1886. [[CrossRef](#)]
27. Dumont, C.; Bourgeois, S.; Fessi, H.; Dugas, P.-Y.; Jannin, V. *In-vitro* evaluation of solid lipid nanoparticles: Ability to encapsulate, release and ensure effective protection of peptides in the gastrointestinal tract. *Int. J. Pharm.* **2019**, *565*, 409–418. [[CrossRef](#)] [[PubMed](#)]
28. Gupta, K.M.; Das, S.; Chow, P.S.; Macbeath, C. Encapsulation of Ferulic Acid in Lipid Nanoparticles as Antioxidant for Skin: Mechanistic Understanding through Experiment and Molecular Simulation. *ACS Appl. Nano Mater.* **2020**, *3*, 5351–5361. [[CrossRef](#)]
29. Chaudhary, A.; Jaswal, V.S.; Choudhary, S.; Sonika, U.; Sharma, A.; Beniwal, V.; Tuli, H.S.; Sharma, S. Ferulic Acid: A Promising Therapeutic Phytochemical and Recent Patents Advances. *Recent Pat. Inflamm. Allergy Drug Discov.* **2019**, *13*, 115–123. [[CrossRef](#)] [[PubMed](#)]
30. Srinivasan, M.; Sudheer, A.R.; Menon, V.P. Ferulic Acid: Therapeutic Potential Through Its Antioxidant Property. *J. Clin. Biochem. Nutr.* **2007**, *40*, 92–100. [[CrossRef](#)] [[PubMed](#)]
31. Danaei, M.; Dehghankhold, M.; Ataei, S.; Hasanzadeh Davarani, F.; Javanmard, R.; Do-khani, A.; Khorasani, S.; Mozafari, M.R. Impact of Particle Size and Polydispersity Index on the Clinical Applications of Lipidic Nanocarrier Systems. *Pharmaceutics* **2018**, *10*, 57. [[CrossRef](#)]
32. Jores, K.; Mehnert, W.; Drechsler, M.; Bunjes, H.; Johann, C.; Mäder, K. Investigations on the structure of solid lipid nanoparticles (SLN) and oil-loaded solid lipid nanoparticles by photon correlation spectroscopy, field-flow fractionation and transmission electron microscopy. *J. Control. Release* **2004**, *95*, 217–227. [[CrossRef](#)]
33. Bhattacharjee, S. DLS, and zeta potential—What they are and what they are not? *J. Control. Release* **2016**, *10*, 337–351. [[CrossRef](#)]
34. Azagury, A.; Baptista, C.; Milovanovic, K.; Shin, H.; Morello, P., III; Perez-Rogers, J.; Goldenshtein, V.; Nguyen, T.; Markel, A.; Rege, S.; et al. Biocoating—A Critical Step Governing the Oral Delivery of Poly-meric Nanoparticles. *Small* **2022**, *18*, 2107559. [[CrossRef](#)]
35. Doktorovova, S.; Souto, E.B. Nanostructured lipid carrier-based hydrogel formulations for drug delivery: A comprehensive review. *Expert Opin. Drug Deliv.* **2009**, *6*, 165–176. [[CrossRef](#)]
36. Wissing, S.A.; Müller, R.H. Solid lipid nanoparticles as carriers for sunscreens: *In vitro* release and *in vivo* skin penetration. *J. Control. Release* **2002**, *81*, 225–233. [[CrossRef](#)]
37. Durán, N.; Teixeira, Z.; Marcato, P.D. Topical Application of Nanostructures: Solid Lipid, Polymeric and Metallic Nanoparticles. In *Nanocosmetics and Nanomedicines: New Approaches for Skin Care*, 1st ed.; Beck, R., Guterres, S., Pohlmann, A., Eds.; Springer: Berlin, Germany, 2011; pp. 69–100.
38. Bunjes, H.; Unruh, T. Characterization of lipid nanoparticles by differential scanning calorimetry, X-ray and neutron scattering. *Adv. Drug Deliv. Rev.* **2007**, *59*, 379–402. [[CrossRef](#)] [[PubMed](#)]

39. Rodenak-Kladniew, B.; Islan, G.A.; de Bravo, M.G.; Durán, N.; Castro, G.R. Design, characterization and *in vitro* evaluation of linalool-loaded solid lipid nanoparticles as a potent tool in cancer therapy. *Colloids Surf. B* **2017**, *154*, 123–132. [[CrossRef](#)] [[PubMed](#)]
40. Tian, H.; Lu, Z.; Li, D.; Hu, J. Preparation and characterization of citral-loaded solid lipid nanoparticles. *Food Chem.* **2018**, *248*, 78–85. [[CrossRef](#)] [[PubMed](#)]
41. Hou, D.; Xie, C.; Huang, K.; Zhu, C. The production and characteristics of solid lipid nanoparticles (SLNs). *Biomaterials* **2003**, *24*, 1781–1785. [[CrossRef](#)]
42. Omwoyo, W.N.; Ogutu, B.; Oloo, F.; Swai, H.; Kalombo, L.; Melariri, P.; Mahanga, G.M.; Gathirwa, J.W. Preparation, characterization, and optimization of primaquine-loaded solid lipid nanoparticles. *Int. J. Nanomed.* **2014**, *9*, 3865–3874. [[CrossRef](#)]